2016 IEEE 19th International Conference on Intelligent Transportation Systems (ITSC)
Windsor Oceanico Hotel, Rio de Janeiro, Brazil, November 1-4, 2016

Fusing directional passive UHF RFID and stereo vision for tag association in outdoor scenarios

D. F. Llorca, R. Quintero, I. Parra, M. Jiménez, C. Fernández, R. Izquierdo, M. A. Sotelo

***Abstract*— Stereo-based object detection systems can be greatly enhanced thanks to the use of passive UHF RFID technology. By combining tag localization with its identification capability, new features can be associated with each detected object, extending the set of potential applications. The main problem consists in the association between RFID tags and objects due to the intrinsic limitations of RSSI-based localization approaches. In this paper, a new directional RSSI-distance model is proposed taking into account the angle between the object and the antenna. The parameters of the model are automatically obtained by means of a stereo-RSSI automatic calibration process. A robust data association method is presented to deal with complex outdoor scenarios in medium sized areas with a measurement range up to 15m. The proposed approach is validated in crosswalks with pedestrians wearing portable RFID passive tags.**

***Index Terms*— RFID-stereo data association, RSSI-distance calibration, stereo-based pedestrian detection, directional RSSI-distance model.**

I. INTRODUCTION

The use of Radio Frequency Identification (RFID) is emerging as one of most fundamental technologies due to its localization and identification capabilities. It has achieved a widespread success in various applications ranging from asset tracking, highway toll collection, supply chain management, animal identification, surveillance systems, aerospace, etc. [1], [2]. More specifically, passive Ultra High Frequency (UHF) technology has attracted a great attention from both industry and academia due to the fact that a built-in power source in the tag is not needed. The passive tag can communicate with the reader thanks to the use of backscattered coupling from the tag to the reader. In addition, by modeling the Received Signal Strength Indicator (RSSI) a rough estimation of the relative position between the tag and the antenna can be obtained. When more than one (non-isotropic) or more than two (isotropic) antennas are available, different multilateration techniques can be applied to compute the global position of the tagged objects (RFID localization). However, the accurate and robust estimation of the physical location of tagged objects is still a challenging task due to the intrinsic limitations and directional dependence when using RSSI as a distance metric [3], [4]. When other sensors are available, different fusion schemes can be used to improve localization [5], [6]. However, if the accuracy of the range measurements given by such other sensors (for example, vision- or laser-based systems) is much better than the one provided by RFID systems, then RFID localization is only used to solve the data association problem, linking tags with objects, and considering the physical location of the tagged object as the one given by the other sensors [7], [8].

D. F. Llorca, R. Quintero, I. Parra, M. Jiménez, C. Fernández, R. Izquierdo and M. A. Sotelo are with the Computer Engineering Department, Polytechnic School, University of Alcalá, Alcalá de Henares, Madrid, Spain. email: david.fernandezl@uah.es.

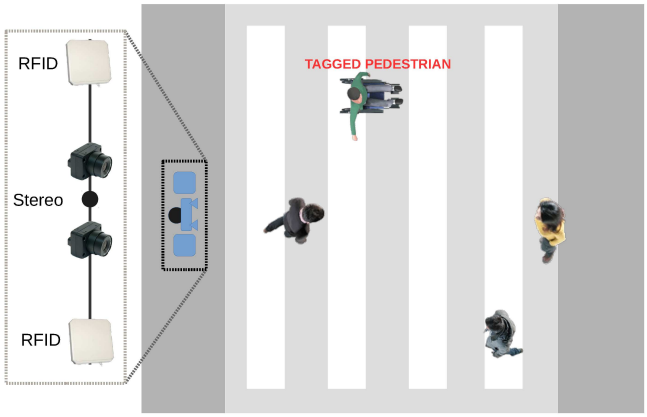

Fig. 1. Pedestrian crossing scenario. Only one (a maximum or two) pedestrians are tagged. The system needs to associate the detected tag with the corresponding pedestrian.

In this paper, a new directional RSSI-distance model is proposed to improve the accuracy and stability of the distance measurements given by a passive UHF RFID system. All the model parameters are automatically obtained by applying an automatic stereo-RSSI calibration process. A robust data association method based on a global nearest neighbor and a new distance metric is presented to deal with complex outdoor scenarios in medium sized areas with a measurement range up to 15m. To validate the proposed approach an intelligent pedestrian crossing application is used as an example (see Fig. 1). A stereo-based pedestrian detection system [9] provides accurate localization of pedestrians that may carry passive and portable RFID tags. The most typical scenario involves several pedestrians crossing, but only one or two carrying a tag. The infrastructure has to estimate the tagged pedestrian among all the tracked pedestrians to efficiently provide an adaptive response to users with disabilities [8].

II. RELATED WORK

Object localization based on radio frequency identification technology has been widely proposed to address a considerable number of different applications [6], including different technologies such as RFID, Ultra-Wide Band (UWB), Bluetooth, BLE, ZigBee, WiFi, etc. [5], and different RSSI-based

978-1-5090-1889-5/16/$31.00 ©2016 IEEE

localization approaches such as multilateration, Bayesian inference, nearest-neighbor and proximity [6]. A considerable number of works have been proposed for the localization of radio-frequency tags (objects) with fixed nodes (antennas), as well as the localization of moving nodes using a fixed set of tags [5]. However, for the course of this work, we focus on the localization of moving passive tags using fixed or moving nodes in combination with vision-based approaches.

In most cases, the combination of wireless sensors and vision-based localization techniques is used to increase the global localization accuracy by means of some Bayesian filter (Kalman Filter -KF-, Extended KF -EKF-, Particle Filter -PF-, Unscented Kalman Filter -UKF-, etc.), that fuses the range measurements coming from the different sensors. Thus, in [10], eight directive RFID antennas, and one camera are embedded on a mobile robot to detect passive tags worn on the user's clothes, in indoor environments with a range of 5m. Saliency maps are obtained for each antenna by counting occurrence frequencies, and translated to the image domain. These maps are used to filter particles on a PF applied over a skin probability image. In [11], RFID-based localization in a small indoor area of interest with a limited number of objects is carried out via RSSI measurements and combined with a camera-based localization by means of an UKF. There is an obvious improvement in the RFID-based localization accuracy thanks to the use of the monocular vision system. The formula between RSSI measurements and distance is adjusted using a manual calibration process. No data association is performed since results are provided only with one object that is directly associated with the detected tag. A similar fusion scheme using a Particle Filter (PF) to combine RSSI data from passive RFID tags with stereo measurements is proposed in [12]. Four different antennas are used to cover an indoor region of 4×4 meters. RSSI-distance calibration procedure involves manual distance computation, and a linear-regression model is used to obtain distance from RSSI measurements. Multilateration is used to perform RSSI-based localization. Again, no data association is applied since only one object is taken into account. PF is also applied in [13] to fuse WiFi and vision measurements in outdoor scenarios. The so-called fingerprints (SSID and RSSI of different nodes) and a GPS are used to perform RSSI-distance calibration. The GPS is only used for calibration, and its accuracy is limited when no differential corrections are available. RSSI-based localization is carried out using the centroid position of all the access points. Data association is not applied since results are obtained using only one person.

An interesting dynamical RSSI-distance calibration process is proposed in [14] using linear local models around the target, combining RSSI and vision measurements using an Extended Information Filter (EIF) in indoor environments. Although the dynamic RSSI model increases localization accuracy, its use is limited to one-object one-tag scenario. In real scenarios with multiple targets, perfect data association will be needed. A room-level accuracy system is proposed in [15], by means of a RSSI-room calibration process and a video tracking system able to detect a person entering/leaving a room. Trilateration is then applied to solve the room-level localization problem. Results are provided with only one candidate so no data association process is applied.

As can be observed, and suggested by [16] and [8], data association problem between objects or blobs and tags has been somehow neglected in the literature, which limits the applicability to real scenarios. In [16] a probabilistic framework to combine RFID and monocular vision measurements for indoor scenarios in a limited range is proposed. A predefined and manual grid is used to perform RSSI-distance calibration, modeling each grid position with a Gaussian distribution. RSSI-based localization is solved by means of a Mixture of Gaussians, where each mode corresponds to one RFID antenna. A Hidden Markov Model is finally applied to deal with the data association problem using a Gaussian distribution as a metric, and finally combining RSSI and vision measurements to compute the person/tag final position.

However, as suggested by several studies [3], [4] there are intrinsic limitations when using RSSI as a distance metric in terms of accuracy and stability for localization purposes. Thus, as in [7], we propose to use the RFID system as an identification tool, and the vision system for localization. Thus the data fusion problem can be translated into a pure data association problem. A global nearest neighbor (GNN) algorithm with a novel distance metric is proposed to link radio frequency tags with stereo objects (pedestrians). Our RSSI-distance calibration process is fully automatic. The system is devised to be used in outdoor scenarios (crosswalks), in medium sized areas with a measurement range up to 15m, which is a clear contribution w.r.t. the state of the art.

III. RSSI-BASED LOCALIZATION

In most RSSI-based localization approaches, the signal strength received by a sensor from another one is considered as a monotonically decreasing function of their distance (standard approach). As described in [4], a simplified form of the relation between distance and receive power has been mostly used:

$$P_r(dBm) = P_{r1}(dBm) - K.log_{10}(D(m)) \quad (1)$$

where P_{r1} is the received power in dBm at $1m$, K is the loss parameter and D is the distance between the receiver and the transmitter. The values of P_{r1} and K are determined by minimizing the root mean square error using calibration data (RSSI and ground-truth distance values). However, the standard approach does not consider the directional (angular) dependence of the signal strength between the antenna and the tags. In order to take into account the radiation pattern of the wireless antennas, a more sophisticated model is proposed, including the angle between the antenna and the user, that is, $P_r(dBm) = f(D, \theta)$. Although the signal strength can be considered as a logarithmically decreasing function of its distance, that is not the case w.r.t. the angle. After analyzing the calibration data we concluded that the signal strength linearly decreases w.r.t. the angle, so we propose to

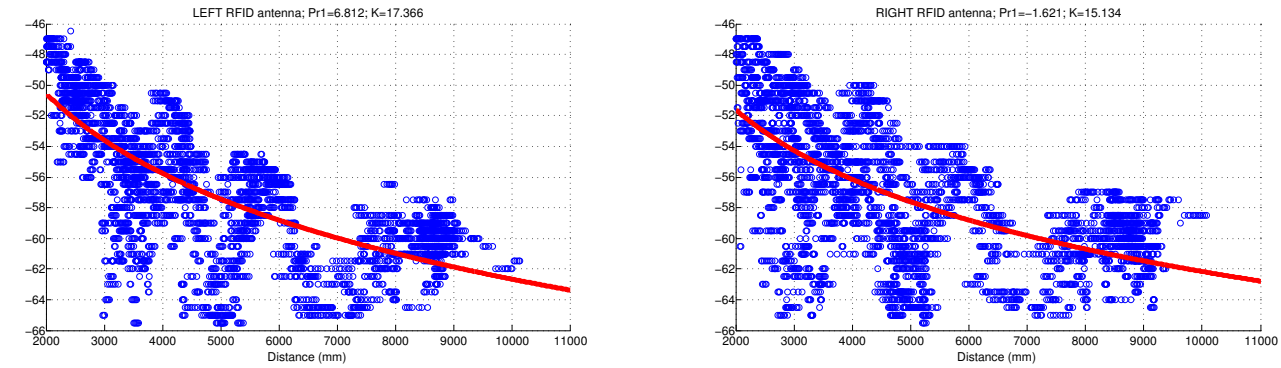

(a)

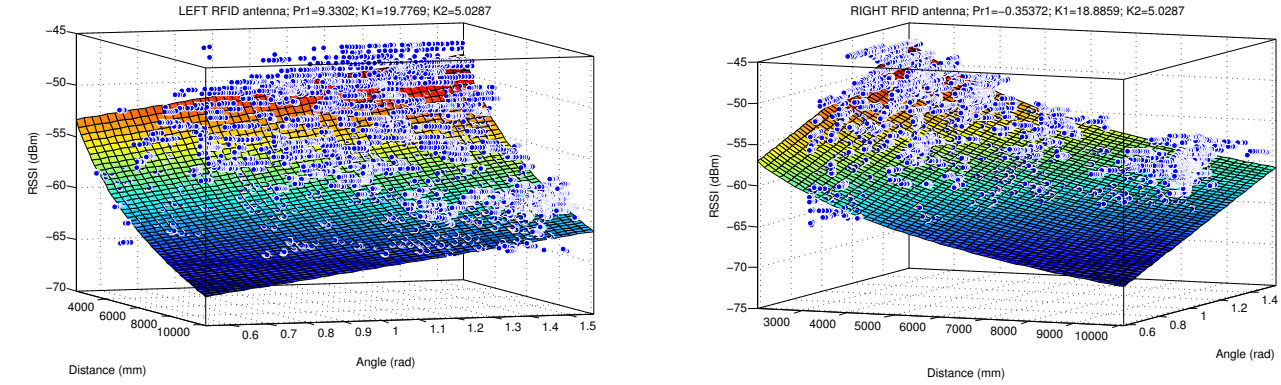

(b)

Fig. 2. (a) Standard and (b) directional RSSI-distance RFID model and calibration data for both left and right antennas.

use a directional form of the relation between distance and receive power as follows:

$$P_r(dBm) = P_{r1}(dBm)K_1.log_{10}(D(m)) + K_2.\theta \qquad (2)$$

where θ is the angle of the relative position between the tag (stereo-based) and its corresponding antenna.

Thanks to the stereo-based object detection system [9] the calibration data including thousands of RSSI, distance and angle measurements can be automatically obtained. Stereo reconstruction provides 3D points P_{LC} referenced to the left camera (LC). The relative positions of both the left and the right antennas (LA; RA) w.r.t. the left camera are approximated by using an identity rotation matrix and translation vectors only containing the X component. Thus, points P_{LA} and P_{RA} can be easily computed and associated with their corresponding RSSI values. By using a sequence of one person carrying one tag in a fixed position and orientation, and moving around the stereo region, the stereo-based pedestrian location system can be applied to get 3D measurements w.r.t. one reference point. These measurements can be directly associated with the RSSI values given by the antennas since data association is not needed at this stage (one person-one tag). The 3D position of the tag w.r.t. the stereo system is approximated as the center of the 3D blob assuming a fixed tag height w.r.t. the road plane.

Thanks to the automatic calibration procedure, non-linear least squares fitting can be applied over data to obtain the parameters of the directional model (P_{r1}, K_1, K_2). For this case, we compute the variance as a function of both the distance and the angle $\sigma^2_{D,\theta}$. These models and their corresponding parameters are showed in Fig. 2, where the standard model is also depicted. Now, for a given RSSI measurement P_{ri} we compute the curve where Eq. 2 intersects the plane $P_r = P_{ri}$, which will represent the potential location of the tag. A Kalman filter is finally used to get steadier distance estimations for each tag and antenna. A constant variation model is used. The state vector includes the RSSI value and its variation, whereas the measurement vector is defined by the RSSI value. The RSSI variance is computed during the calibration process.

IV. Stereo-RSSI Data Association

In the standard approach (non-directional) [8], a single RSSI value yields a sphere with the antenna position at its center and radius equal to the RSSI-based distance measurement as possible tag locations. In our case, a fixed and known tag height is assumed to reduce the 3D sphere to a 2D circumference. Then the tag position can be determined by intersecting the circumferences generated by each antenna. For isotropic antennas with a 360° radiation pattern, a minimum of 3 antennas are needed to compute the tag

location. However, in our case, directional 180° antennas are used and one of the intersection points can be discarded. Accordingly, two antennas are enough for providing a unique solution. A similar reasoning can be used for the directional case, in which the tag fixed height assumption provides 2D curves that should intersect at a unique point.

However, as suggested by previous works [3], [4], and supported by our data, the intrinsic limitations when using RSSI as a distance metric in terms of accuracy and stability, as well as, in our case, the suboptimal position of both antennas (at the same baseline) causes that the intersection point or area (including the uncertainties) is not a robust and accurate metric to be used for solving the data association problem. Accordingly, a new distance metric that models the probability of association between a 3D object (stereo-based) and a detected tag (RSSI-based) is proposed.

The distance d_k^{ij} between a 3D object i and the tag j (assuming fixed height) detected by antenna k ($k = LA$ for left antenna and $k = RA$ for right antenna) is modeled using a univariate normal distribution where the mean value is the RSSI-based computed distance d_k^j, the variance is the one computed after RSSI-distance calibration $\sigma^2_{d_k^j}$ (standard) or $\sigma^2_{d_k^j,\theta}$ (directional) and the independent variable is the 3D object position w.r.t. the antenna $d^i_{stereo,k}$:

$$d_k^{ij} = \frac{1}{\sigma_{d_k^j,\theta}\sqrt{2\pi}} e^{-\frac{(d^i_{stereo,k} - d_k^j)^2}{2\sigma^2_{d_k^j,\theta}}} \tag{3}$$

Note that Eq. (3) can be valid for both the standard and the directional approach, assuming that $\theta = 0$ for the standard model. The graphical representation of this metric is depicted in Fig. 3 for the standard approach. For the directional case, the curves resulting from the intersection between the directional model and the RSSI plane will be used instead of circumferences.

Eq. (3) is computed for both antennas. If one of them does not receive signal, the metric would be set to zero. In order to compute the global metric d^{ij} that represents the probability that tag j is being worn by person i, the following equation would be applied:

$$d^{ij} = d^{ij}_{LA} . d^{ij}_{RA} \tag{4}$$

This approach can be easily extended to N antennas by applying the following equation:

$$d^{ij} = \prod_{k=1}^{N} d_k^{ij} \tag{5}$$

To achieve a reliable data association, a global nearest-neighbor (GNN) [17] algorithm is applied. The association probability between the predicted position of all pedestrians ($i = 1 \ldots P$) and all the detected tags ($j = 1 \ldots TB$) are computed at each time iteration t. The corresponding probability matrix C is defined using the computed distances d^{ij}. The Hungarian or Munkres algorithm is then applied so that the

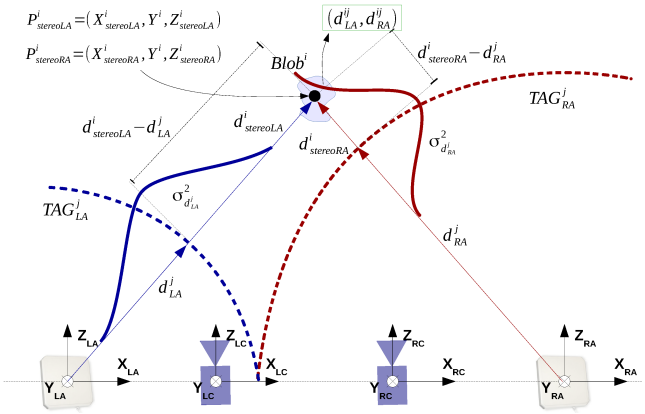

Fig. 3. Graphical representation of the new metric defined between a 3D object and the tag detected by both antennas.

global association probability is maximized, as long as the final assignment is always greater than 0.5 (higher thresholds can not be used due to the unstable RSSI measurements). In order to avoid oscillations between the associations, a variable c^{ij} is used for each 3D object i accounting the number of times it has been associated with tag j. The final association at time t is given by the 3D object i that holds the maximum number of associations. When this counter achieves a maximum threshold, the association is fixed until the tag or the 3D object leaves the detection area.

V. Experimental Results

The experimental setup is is depicted in Fig. 4-left. On the one hand, the stereo platform is composed of two CMOS USB cameras with VGA resolution and a baseline of 30cm, with automatic gain control, with two optics with a focal length of 2.8mm (wide angle). A specific synchronization HW controls both the external trigger and the shutter between the cameras. On the other hand, an UHF Class 1 Gen 2 RFID Speedway Revolution R220 reader with two inputs is connected to the Ethernet card of the PC. Two far field circularly polarized panel antennas within the 865-870MHz band (Europe frequency allocation) are connected to the reader. Due to our range needs in outdoor scenarios, and after some experimental work testing different passive tags (see Fig. 4-right) the Onmi-ID Dura 3000 RFID passive tag was selected, which have a theoretical read range up to 20m.

The stereo-based object detection system developed by our group, has been previously validated in different types of scenarios [8] (daytime and nighttime), with an average Detection Rate (DR) of 99% at a False Positive Rate (FPR) of 1.5%. In addition, the 90% of the objects detected by the system were tracked in less than 10 frames after they were fully visible (0.33 seconds).

In order to validate the proposed methodology, different types of sequences have been recorded in a crosswalk scenario, including different number of people, tags and trajectories. Some users were required to carry one tag at a fixed height and pointing to the antennas. Other users were

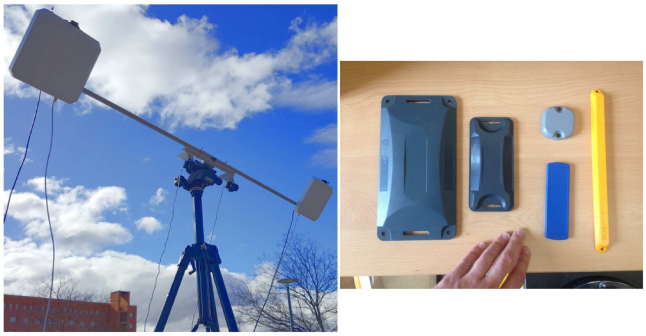

Fig. 4. Left: sensor setup, including two CMOS USB cameras and two far field circularly polarized panel antennas within the 865-870MHz band (Europe frequency allocation) located at the same baseline. Right: different passive RFID tags used in our experiments.

only required to cross the road as usual. In order to validate the proposed methodology, the following metrics are used: percentage of time that the tag is correctly associated (CA, Correct Association) and percentage of time a tag has not been associated (NA, Not Associated). Due to the nature of our problem, a tag associated to a wrong pedestrian for cases in which the pedestrian is really close to the tagged one can be considered as correct associations. Accordingly, we also compute the percentage of time the tag is correctly associated or associated to a near pedestrian walking or waiting in parallel (CNA, Correct-Near Association). In addition, we have measured the average association delay (D, Delay), that is, the average number of frames that the system needs for correctly associating each detected tag with its corresponding 3D object. Note that the system is currently running at 25Hz, so we can easily convert D to time in seconds.

We provide results corresponding to the standard approach and the directional one in Table I. As can be observed the directional approach outperforms the results given by the standard one in most cases. Thus, CA increases a $6,9\%$ for sequences in which one tagged and one non-tagged pedestrian cross in parallel, a $8,4\%$ for cases where two tagged pedestrians cross in opposite directions, a $5,5,\%$ for sequences where two tagged pedestrians cross in parallel, and a $5,7\%$ in cases where there is one tagged pedestrian among five non-tagged ones in mixed conditions. In addition, the average delay considerably decreases for those cases. The increase on CA metric is mainly due to the superior performance of the directional model when associating the RFID tag between close pedestrians crossing in parallel. However, the better lateral discrimination capacity of the directional model does not involve a considerable increase in CNA metric, which on average is only $0,4\%$ better for the directional model than for the standard approach.

Considering all the sequences, average metrics are: $CA_{Std} = 74,8\%$, $CA_{Dir} = 78,0\%$, $CNA_{Std} = 81,1\%$, $CNA_{Dir} = 81,5\%$, $NA_{Std} = 14,7\%$, $NA_{Dir} = 12,9\%$, $D_{Std} = 48,7$ frames, $D_{Dir} = 43,7$ frames. Accordingly the overall increase of the directional model in CA and CNA metrics is $3,2\%$ and $0,1\%$ respectively. In addition, the overall decrease in NA and D metrics is $1,8\%$ and 5 frames respectively.

Different examples are depicted for both the standard and the directional approach in Figs. 5(a) and 5(b) respectively. The upper row shows the images of the left camera with a color-coded square that represents the associated tag nearby to the detected pedestrian. The lower row depicts the XZ-map (bird's eye view) without road points, including the detected blobs and the corresponding RSSI circumferences or curves for each antena depending on the model (standard or directional). Each RFID tag is labeled with a different color (green or blue). As can be observed, in most cases the RSSI curves of the directional model are closer to the tagged pedestrian than the RSSI circumferences of the standard approach. In the third example the standard approach incorrectly associates each tag for two tagged-pedestrians crossing and in the fourth example the model is not able to correctly associate one of the tags to its corresponding pedestrian.

VI. Conclusions

In this paper we have presented a novel directional RSSI-distance model to enhance the localization performance of standard methods that do not take into account the angle between the passive tag and the antennas. All the parameters of the directional passive UHF RFID model are obtained by using a stereo-based object detection system that allows the implementation of a fully automatic RSSI-distance calibration process. Then, a robust data association procedure is presented. A new probabilistic metric is used along with a global nearest neighbor (GNN) algorithm to associate each detected tag with its corresponding object, in outdoor scenarios with a measurement range up to 15m, where the number of non-tagged object is usually larger than the number of tagged ones. Specifically, to validate the proposed approach, an intelligent pedestrian crossing application is presented. Results showed that the directional model enhances the lateral discrimination capability of the system and reduces the association delay.

Future works will involve exploring other active but low cost radio frequency identification technologies such as Bluetooth Low Energy (BLE) to enhance the association between tags and objects, increasing the range and improving the stability of the RSSI. In addition, other application scenarios will be explored including indoor environments.

VII. Acknowledgments

This work was supported by Research Grants DPI2014-59276-R (Spanish Ministry of Economy), SPIP2014-1300 and SPIP2015-01737 (General Traffic Division of Spain) and SEGVAUTO-TRIES-CM S2013/MIT-2713 (Community of Madrid).

References

[1] B. Nath, F. Reynolds, and R. Want, "Rfid technology and applications." *IEEE Pervasive Computing*, vol. 1, pp. 22–24, 2006.

[2] S. B. Miles, S. E. Sarma, and J. R. Williams, *RFID technology and applications*. Cambridge University Press, 2008.

TABLE I

STEREO-RSSI DATA ASSOCIATION RESULTS.

Sequence Description	**Duration (frames)**	**CA (%) Std. / Dir.**	**CNA (%) Std. / Dir.**	**NA (%) Std. / Dir.**	**D (frames) Std. / Dir.**
Calibration	8230	99,4 / 99,5	99,4 / 99,5	0,6 / 0,5	22,0 / 5,0
One Tagged Pedestrian Crossing	3270	87,5 / 87,6	87,5 / 87,6	12,5 / 12,4	35,0 / 34,8
One Tagged / One Non-tagged Pedestrians Opposite Crossing	2710	67,0 / 67,0	67,0 / 67,0	33,0 / 33,0	94,0 / 93,8
One Tagged / One Non-tagged Pedestrians Paralell Crossing	2380	68,3 / 75,2	76,5 / 77,7	23,5 / 22,3	60,0 / 57,5
One Tagged / Two Non-tagged Pedestrians Mixed	4740	57,1 / 59,5	84,2 / 77,8	14,4 / 13,1	52,0 / 44,3
Two Tagged Pedestrians Opposite Crossing	1270	59,6 / 68,0	59,6 / 68,0	35,1 / 32,0	48,8 / 43,0
Two Tagged Pedestrians Paralell Crossing	1250	58,1 / 63,7	58,1 / 63,7	41,9 / 36,3	46,9 / 31,9
One Tagged / Five Non-tagged Pedestrians Mixed	9180	62,6 / 68,3	75,5 / 74,6	8,7 / 5,2	31,0 / 39,6

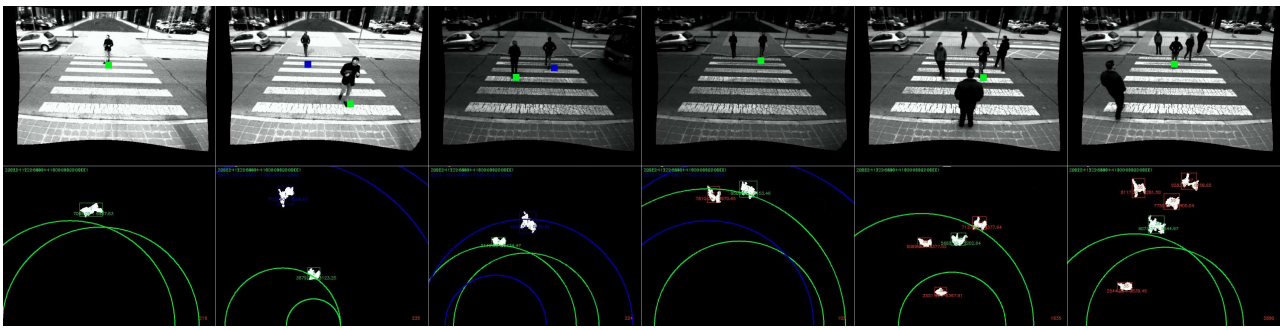

(a)

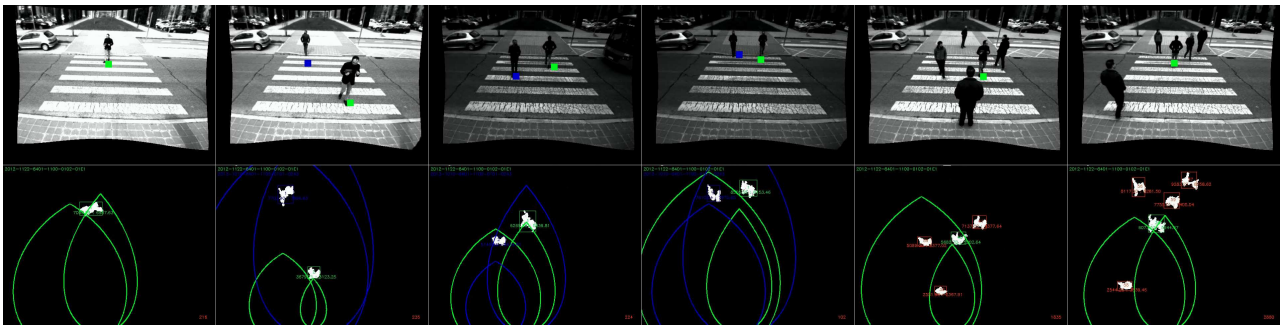

(b)

Fig. 5. (a) Standard and (b) directional results. Upper row: left image with color-coded identification (squares). Lower row: XZ-map (top-view without road points), detected blobs and RSSI circumferences/curves. Each tag is labeled with a different color (green or blue).

[3] A. T. Parameswaran, M. I. Husa, and S. Upadhyaya, "Is rssi a reliable parameter in sensor localization algorithms an experimental study," in *Field Failure Data Analysis Workshop*, 2009.

[4] K. Heurtefeux and F. Valois, "Is rssi a good choice for localization in wireless sensor network?" in *IEEE 26th International Conference on Advanced Information Networking and Applications (AINA)*, 2012.

[5] H. Liu, H. Darabi, P. Banerjee, and J. Liu, "Survey of wireless indoor positioning techniques and systems," *IEEE Transactions on Systems, Man and Cybernetics - Part C*, vol. 37, no. 6, pp. 1067–1080, 2007.

[6] J. Zhou and J. Shi, "Rfid localization algorithms and applicationsa review," *Journal of Intelligent Manufacturing*, vol. 20, no. 6, pp. 695–707, 2009.

[7] A. Isasi, S. Rodriguez, J. L. D. Armentia, and A. Villodas, "Location, tracking and identification with rfid and vision data fusion," in *2010 European Workshop on Smart Objects: Systems, Technologies and Applications (RFID Sys Tech)*, 2010.

[8] D. F. Llorca, R. Quintero, I. Parra, R. Izquierdo, C. Fernndez, and M. A. Sotelo, "Assistive pedestrian crossings by means of stereo localization and rfid anonymous disability identification," in *IEEE Intelligent Transportation Systems Conference (ITSC)*, 2015.

[9] D. F. Llorca, I. Parra, R. Quintero, C. Fernández, R. Izquierdo, and M. A. Sotelo, "Stereo-based pedestrian detection in crosswalks for pedestrian behavioural modelling assessment," in *ICINCO2014, International Conference on Informatics in Control, Automation and Robotics*, 2014.

[10] T. Germa, F. Lerasle, N. Ouadah, and V. Cadenat, "Vision and rfid data fusion for tracking people in crows by a mobile robot," *Computer Vision and Image Understanding*, vol. 114, pp. 641–651, 2010.

[11] T. Nick, S. Cordes, J. Gotze, and W. John, "Camera-assisted localization of passive rfid labels," in *International Conference on Indoor Positioning and Indoor Navigation*, 2012.

[12] F. Schwiegelshohn, T. Nick, and J. Gotze, "Localization based on fusion of rfid and stereo image data," in *10th Workshop on Positioning Navigation and Communication (WPNC)*, 2013.

[13] T. Miyaki, T. Yamasaki, and K. Aizawa, "Tracking persons using particle filter fusing visual and wi-fi localizations for widely distributed camera," in *IEEE International Conference on Image Processing (ICIP)*., 2007.

[14] A. de San Bernabe, J. R. M. d. Dios, and A. Ollero, "Mechanisms for efficient integration of rssi in localization and tracking with wireless camera networks," in *IEEE/RSJ International Conference on Intelligent Robots and Systems (IROS)*, 2013.

[15] L. Radaelli, Y. Moses, and C. S. Jensen, "Using cameras to improve wi-fi based indoor positioning," *Lecture Notes in Computer Science*, vol. 8470, pp. 166–183, 2014.

[16] M. Goller, C. Feichtenhofer, and A. Pinz, "Fusing rfid and computer vision for probabilistic tag localization," in *IEEE International Conference on RFID (IEEE RFID)*, 2014.

[17] S. Blackman and R. Popoli, *Design and analysis of modern tracking systems*. Artech House, 1999.